ADVANCED FUNCTIONAL MATERIALS
www.afm-journal.de

Cerium-Based Metal–Organic Framework with Intrinsic Haloperoxidase-Like Activity for Antibiofilm Formation

*Zijun Zhou, Sirong Li, Gen Wei, Wanling Liu, Yihong Zhang, Chenxin Zhu, Shujie Liu, Tong Li, and Hui Wei**

Biofilms adhering to surfaces have severe impacts on both public health and industry. Environmentally friendly strategies for combating biofilms are needed due to the biosafety issues brought by traditional commercial anti-biofilm additives. Enzyme-based strategies for biofilm treatment have attracted great research interest, but there is still a major challenge ahead due to the high economic cost and limited stability of natural enzymes. Inspired by the antifouling mechanism of natural haloperoxidase (HPO) secreted by marine algae, which catalyzes the oxidative bromination of bacterial quorum sensing signaling molecules, its artificial enzyme is proposed here in response to the situation mentioned above. A cerium-based metal–organic framework (Ce-MOF) is verified to possess HPO-like activity. Based on its favorable enzyme-like activity, the Ce-MOF exhibits remarkable antibacterial and biofilm formation suppression abilities. This study not only expands the variety of HPO-like artificial enzymes but also paves the way for the application prospect of Ce-MOFs in water pipe cleaning and biofouling treatment.

1. Introduction

Surface-adhered biofilms, the aggregates of micro-organisms, shelter, and nourish the bacteria, being 10–1000 times more resistant to antibiotics compared with planktonic mode, the other mode of bacterial growth.[1] Biofilms adhering onto different surfaces tend to cause severe consequences both in the fields of industry and healthcare, including water[2] and food contamination,[3] marine biofouling,[4] and infectious diseases.[5] Current treatments for surface-adhered biofilms can be categorized into three types. The first one is mainly based on surface performances,[6] including surface chemistry modifications[7] and construction of specific topography,[8] both of which are designed for biofilm prevention but are unable to eliminate the formed biofilm. Utilizing bactericidal materials is another method for biofilm inhibition.[9] However, it has been proved to cause environmental problems, like unexpected harm to non-target organisms, and to have little effect on established biofilm eradication.[6a] Learning from nature, the enzyme-based strategy is more efficient, green, and environmentally friendly.[6a,10] In spite of their high catalytic efficiency, the low stability and high cost of natural and recombinant enzymes limit their applications. Consequently, research focused on materials with enzyme-like activity for biofilm inhibition has arisen. Particularly, nanozymes, the enzyme-like nanomaterials, have received considerable attention,[11] embracing oxidoreductase and hydrolase mimics to treat biofilms.[12] Oxidase and peroxidase mimics can catalyze the oxidation process of oxygen (O_2) and hydrogen peroxide (H_2O_2) into corresponding reactive oxygen species, like singlet oxygen ($^1O_2$), superoxide anion radicals ($O_2^{\bullet-}$), and hydroxide radicals (•OH), which further induce bacterial death.[13] Hydrolase mimics play a pivotal role in degradation of extracellular polymeric substances (EPSs), the self-produced matrix by bacteria in biofilms, consisting of extracellular DNA, proteins, lipids, and polysaccharides.[1c,13b,14] Most of the strategies based on the enzyme mimicking mentioned above possess the anti-biofilm ability by killing individual bacterium or degrading EPSs, while few of them focus on restraining bacterial cell-to-cell communications.

Quorum sensing (QS), the mechanism of bacterial communications, is responsible for bacterial group behaviors (e.g., biofilm formation, bioluminescence, and toxin production).[15] The QS process relies on a series of signaling molecules, among which *N*-acyl homoserine lactones (AHLs) are used by Gram-negative bacteria. AHLs have been found to lose their functions by oxidative halogenation reactions in the presence of hypohalous acids, resulting in quorum quenching (QQ) and further preventing biofilm formation. Since vanadium haloperoxidase (V-HPO), secreted by marine algae,[16] can catalyze the conversion of halide ions (Cl^-, Br^-, and I^-) to their corresponding hypohalous acids (HClO, HBrO, and HIO) in the presence of

Z. Zhou, S. Li, G. Wei, W. Liu, Y. Zhang, C. Zhu, S. Liu, T. Li, H. Wei
College of Engineering and Applied Sciences
Nanjing National Laboratory of Microstructures
Jiangsu Key Laboratory of Artificial Functional Materials
Nanjing University
Nanjing, Jiangsu 210023, China
E-mail: weihui@nju.edu.cn
H. Wei
State Key Laboratory of Analytical Chemistry for Life Science
School of Chemistry and Chemical Engineering
Chemistry and Biomedicine Innovation Center (ChemBIC)
Nanjing University
Nanjing, Jiangsu 210023, China
The ORCID identification number(s) for the author(s) of this article can be found under https://doi.org/10.1002/adfm.202206294.

DOI: 10.1002/adfm.202206294

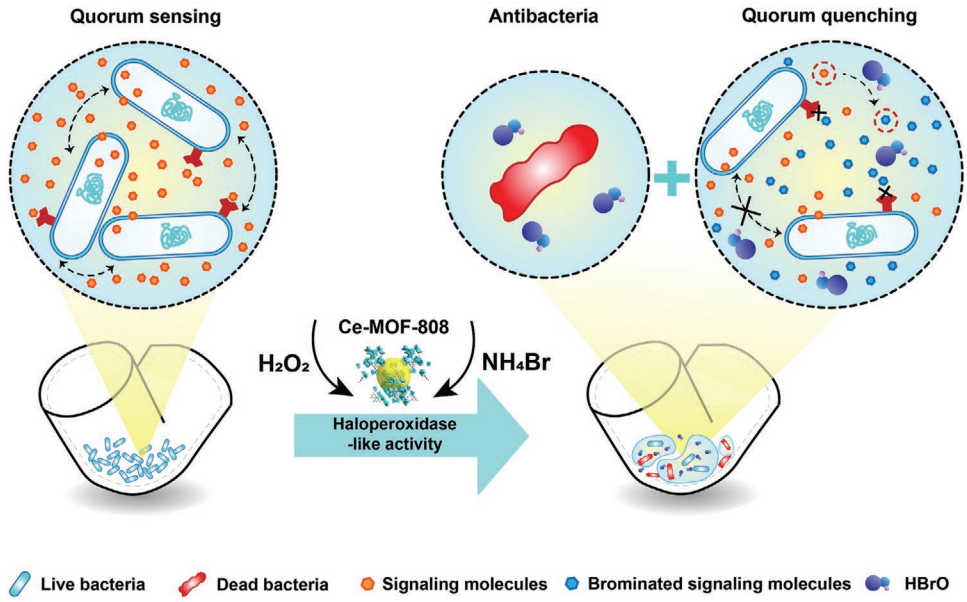

Scheme 1. Schematic illustration of Ce-MOF-808 for antibacteria and inhibiting the formation of biofilms based on its HPO-like activity.

H_2O_2,[17] V-HPO has been used to suppress biofilm formation by QQ.[18] Inspired by the V active sites of most natural HPOs, V-based metal oxides and composites have been employed to mimic HPOs. However, these HPO mimics raise concerns about the toxicity of V.[19] In this juncture, researchers turned to exploring other metal-based materials, of which CeO_2 nanorods (NRs) with remarkable HPO-like activity stood out.[20] Based on this, we reasoned that Ce-containing materials should be ideal mimics for HPO mimicking due to their Ce^{3+}/Ce^{4+} redox potential and biocompatibility.[20,21]

In regard to the outstanding QS obstruction and biofilm formation hindrance ability of HPO, we aimed to develop a new Ce-based material to mimic HPO for surface-adhered biofilm governance. A metal–organic framework (MOF) was selected as the model material for HPO mimicking since MOF is an ideal enzyme analog for its primary and secondary coordination environments, which are similar to those of natural enzymes.[22] Herein, we first proposed that a facilely synthesized Ce-based MOF was able to mimic HPO, catalyzing HBrO generation with favorable antibacterial and QQ abilities (**Scheme 1**). Ce-MOF was demonstrated to endow a great potential both in bactericidal and surface-adhered biofilm formation inhibition applications. In addition to diversifying the variety of HPO mimicries, this work enables their further applications in biofilm-related biofouling, contamination, and infection treatments.

2. Results and Discussion

2.1. Synthesis and Characterizations of Ce-MOF-808

Ce-MOF-808 was synthesized by adding an aqueous solution of $Ce(NH_4)_2(NO_3)_6$ and organic ligand H_3BTC into a mixture of N,N-dimethylformamide and formic acid and heating in an oil bath pan under stirring for 45 min. Three aliquots of the reaction solution were taken out successively every 15 min, named as Ce-MOF-808-15, Ce-MOF-808-30 and Ce-MOF-808-45, for further centrifugation, washing, and drying. To optimize the synthetic time, powder X-ray diffraction (PXRD) was used for characterization, which illustrated that the crystal structures of Ce-MOF-808-15 and Ce-MOF-808-30 were consistent with the standard crystal structure, while Ce-MOF-808-45 was not (Figure S2a, Supporting Information). There was no obvious difference between the HPO-like activity of Ce-MOF-808-15 and that of Ce-MOF-808-30 according to Figure S2b (Supporting Information). Ce-MOF-808-15 was selected for the following studies since it required a shorter synthetic time.

The synthesized Ce-MOF-808-15 was further confirmed by transmission electron microscopy (TEM) and scanning electron microscopy (SEM) images in **Figure 1**a and Figure S1 (Supporting Information), respectively, showing an irregular flocculence morphology. By calculating the peak area proportions of Ce^{3+} and Ce^{4+} in the Ce 3d X-ray photoemission spectroscopy (XPS) spectrum (Figure 1c), the valence of Ce in Ce-MOF-808 was 3.63, while it was 3.79 in CeO_2 NRs (Figure S5 and Table S1, Supporting Information).

As shown in Figure 1d, *Escherichia coli* (*E. coli*), *Staphylococcus aureus* (*S. aureus*), and *Pseudomonas aeruginosa* (*P. aeruginosa*) were negatively charged, while the zeta potential of Ce-MOF-808 was 39.9 ± 1.35 mV. This might facilitate a good interaction between Ce-MOF-808 and negatively charged bacteria and lead to a promising biofilm inhibition effect.[23] The nitrogen adsorption isotherm of Ce-MOF-808 was measured, and the data indicated that its pore width was ≈1.3 nm and its Brunauer–Emmett–Teller (BET) surface area (S_{BET}) was 418.027 $m^2\ g^{-1}$ (Figure 1e). Taken together, the pore width might facilitate the substrate diffusion and the decent S_{BET} of Ce-MOF-808 might contribute to its favorable catalytic activity due to the exposure of multiple active sites, hence leading to the good biofilm inhibition ability.

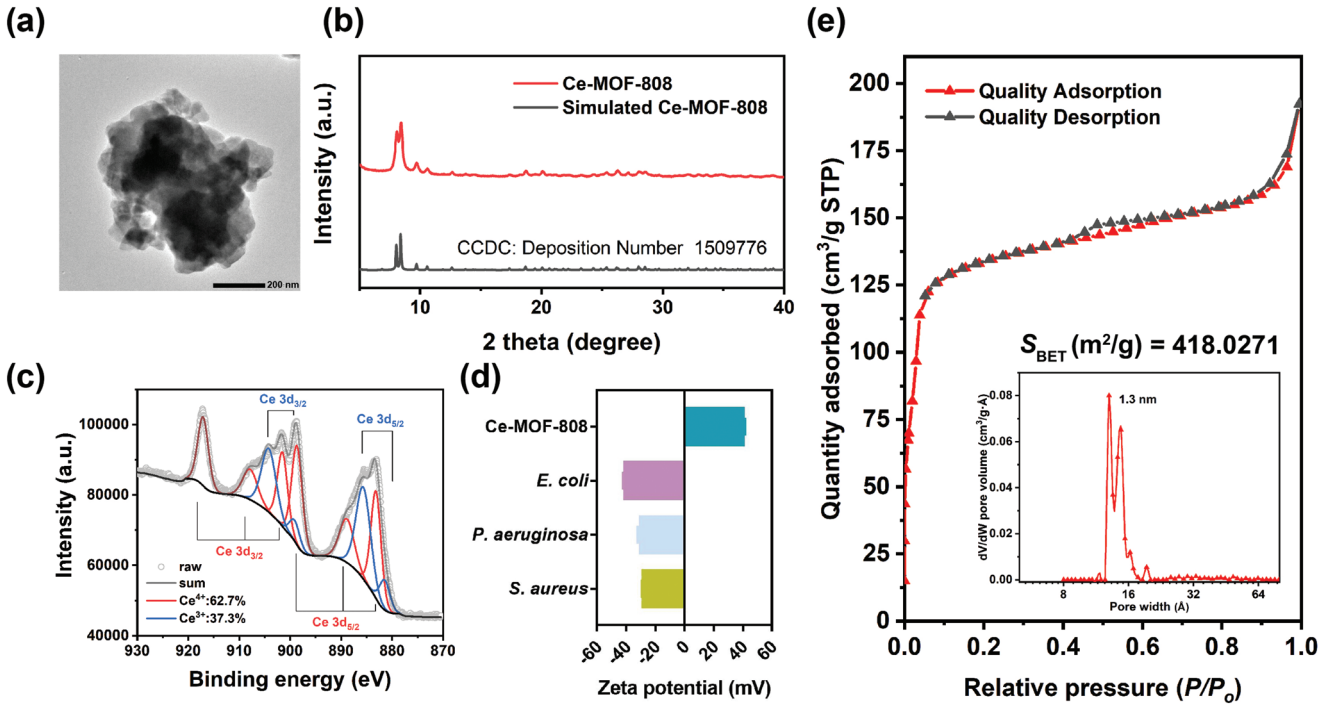

Figure 1. Characterizations of Ce-MOF-808. a) TEM image of Ce-MOF-808. b) XRD patterns of Ce-MOF-808 and simulated Ce-MOF-808. c) Ce 3d XPS spectrum of Ce-MOF-808. d) Zeta potentials of Ce-MOF-808, *E. coli*, *P. aeruginosa* and *S. aureus* in water. e) N_2 adsorption–desorption isotherm curve of Ce-MOF-808. The inset graph shows the pore distribution of Ce-MOF-808.

2.2. Haloperoxidase-Like Activity of Ce-MOF-808

HPO is capable of catalyzing the transformation of organic substrates, such as phenol red (PR), to their corresponding halogenated counterparts in the presence of H_2O_2 and halide ions, accompanied by color changes. PR is also an acid–base indicator, appearing yellow in an acidic solution with a maximum absorption at 443 nm, while its brominated product Br_4PR is bluish violet with a maximum absorption at 590 nm[24] (**Figure 2**a; Figure S3a–c, Supporting Information). The color of the PR solution is rose red under alkaline conditions with a maximum absorption at 559 nm (Figure S3a,f,g, Supporting Information). Therefore, a PR bromination assay was used to investigate the HPO-like activity of Ce-MOF-808. In this assay, NH_4Br served as the Br^- donator and H_2O_2 was another substrate for triggering the oxidative bromination process.

First, to investigate the optimal pH, buffers with different pH values varying from 4.0 to 10.0 were prepared. Digital images of reaction solutions before and after treatments in Figure S3a (Supporting Information) revealed that except for the pH 4.0 group, the colors of the after-treatment reaction solutions under acidic conditions changed obviously, but it is difficult to distinguish the color change in alkaline groups. Figure S3b–g (Supporting Information) shows the UV–vis spectra of the reaction solutions before and after treatments in buffers with different pH values, demonstrating that Ce-MOF-808 was more active under acidic conditions than under neutral and alkaline conditions, with the highest HPO-like activity at pH 5.5. Under alkaline conditions, the peaks at 559 nm decreased slightly, illustrating that Ce-MOF-808 could still convert PR to Br_4PR at alkaline pH, but the activity was too weak to distinguish (Figure S3f,g, Supporting Information). For pH 7.0–7.5, the maximum absorbance of Br_4PR at 571 and 564 nm increased slightly but the activity was also weaker than that under acidic conditions (Figure S3d,e, Supporting Information). As shown in Figure 2f, Ce-MOF-808 was further confirmed to possess the highest activity at pH 5.5. As a result, the following PR bromination assays for HPO-like activity analysis were carried out in sodium acetate–acetic acid buffer at pH 5.5.

Figure 2b illustrates the time-dependent HPO-like activity of Ce-MOF-808 from 0 to 26 h. The peak of Br_4PR at 590 nm increased over time, while the peak of PR at 443 nm decreased, meaning that the oxidative bromination process continued over time, which further confirmed the HPO-like activity of Ce-MOF-808. It took almost 24 h to completely convert PR to Br_4PR. Furthermore, the higher the concentration of H_2O_2 was, the better the HPO-like activity of Ce-MOF-808 was, showing a H_2O_2 concentration dependence (Figure 2c). This H_2O_2 concentration dependence provides Ce-MOF-808 with a potential possibility for H_2O_2 detection. To investigate the stability of Ce-MOF-808, the HPO-like activity of newly synthesized Ce-MOF-808 and Ce-MOF-808 stored at room temperature for 8 months was compared. Consequently, the relative activity of Ce-MOF-808 stored for 8 months remained basically unchanged, illustrating that Ce-MOF-808 was quite stable for a long period of storage (Figure 2d). Then, we carried out 13 groups of control experiments to verify that the oxidative bromination reaction only occurred when Br^-, H_2O_2, Ce-MOF-808, and PR were present at the same time (Figure 2e). In other words, PR was turned into its brominated counterpart

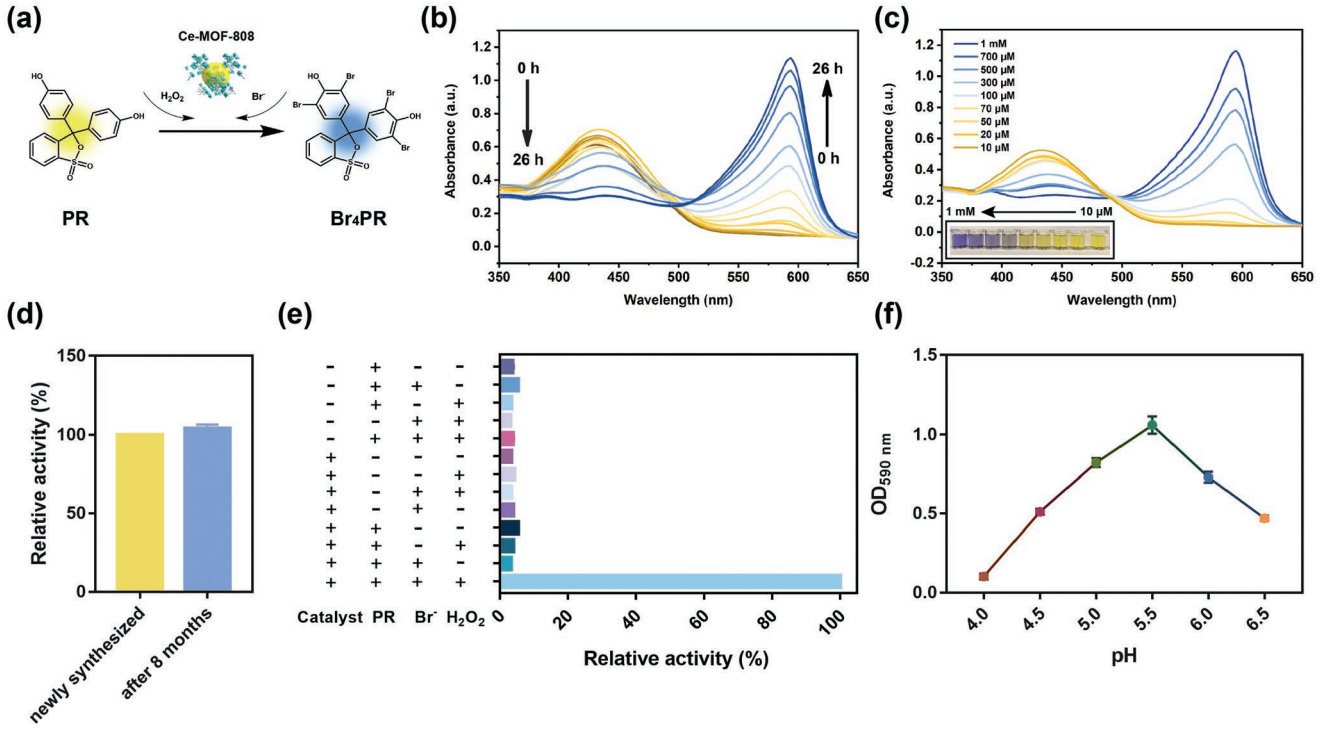

Figure 2. HPO-like activity of Ce-MOF-808. a) Schematic illustration of the oxidative bromination of phenol red (PR) to bromophenol blue (Br_4PR) by Ce-MOF-808. b) Time-dependent UV-vis spectra of the oxidative bromination reaction catalyzed by Ce-MOF-808. c) UV-vis spectra of the oxidative bromination reaction varied by different concentrations of H_2O_2. The inset picture shows that the color of the reaction solution changed from yellow to bluish violet (from right to left) as the concentration of H_2O_2 increased from 10×10^{-6} M to 1×10^{-3} M. d) Comparison of relative HPO-like activity of Ce-MOF-808 stored for different time periods normalized to the activity of the newly synthesized catalyst. e) Control groups of the oxidative bromination reaction. (f) Optimization of pH of the oxidative bromination reaction medium.

by the HPO-like activity of Ce-MOF-808, rather than for other reasons.

Since V_2O_5 nanowires (NWs) and CeO_2 NRs are two of the few materials with HPO-like activity reported thus far and are quite appealing to the marine antifouling field, we further compared their HPO-like activity with Ce-MOF-808 under acidic conditions. The XRD patterns and TEM images in Figure S4 (Supporting Information) confirmed the successful synthesis. Figure S4d (Supporting Information) is an HPO-like activity comparison histogram, showing comparable activity between Ce-MOF-808 and CeO_2 NRs, while V_2O_5 NWs exhibited little activity at pH 5.5. Similar results were also observed in 0.9% NaCl medium (Figure S7b, Supporting Information). However, none of them showed HPO-like activity at pH 8.0 (Figure S7c,d, Supporting Information). Additionally, all of these HPO-like materials were recycled at least 3 times (Figure S6, Supporting Information). Despite a slightly weaker activity than that of CeO_2 NPs, Ce-MOF-808, which is more easily synthesized without any modifications, might be a new, decent biomimetic material possessing HPO-like activity, expanding the variety of materials mimicking HPO.

2.3. Antibacterial Ability of Ce-MOF-808

As a kind of reactive halogen species, HBrO is highly oxidative and hence maintains the bactericidal effect.[21] Considering this, we carried out the following study to evaluate the broad-spectrum antibacterial activity of Ce-MOF-808. *E. coli* and *S. aureus* were used as representatives of Gram-negative bacteria and Gram-positive bacteria, respectively. Considering that *P. aeruginosa* is a typical pathogen in nature, especially in water and air, which forms biofilms and causes water pollution in potable water systems, we also utilized *P. aeruginosa* for antibacterial and antibiofilm studies. As shown in **Figure 3**d, it is obvious that the colony numbers of both Gram-negative and Gram-positive bacteria treated with Ce-MOF-808 in the standard groups were much lower than those in the other three control groups. HBrO generated by the catalysis process of Ce-MOF-808 displayed a better bactericidal effect on Gram-negative bacteria than on Gram-positive bacteria, mainly due to the thinner cell wall of the former.[25] Therefore, the antibacterial effect on *P. aeruginosa* was the best among these three kinds of bacteria. Figure 3a–c shows the histograms of the colony forming counting, quantitating the colonies number on agar plates. It is worth noting that Ce-MOF-808 itself also had weak antibacterial activity toward *P. aeruginosa* and *S. aureus*, according to the results of the ctrl 3 groups (bacteria + Ce-MOF-808). The opposite potentials between Ce-MOF-808 and bacteria might assist in the electrostatic adsorption of Ce-MOF-808 on bacteria and enhance the bactericidal process (Figure 1d). Further bacterial morphological observation via SEM verified that the rough, wrinkled and ruptured bacterial cells indicated by red arrows in Figure S11 (Supporting Information) were solid evidence for

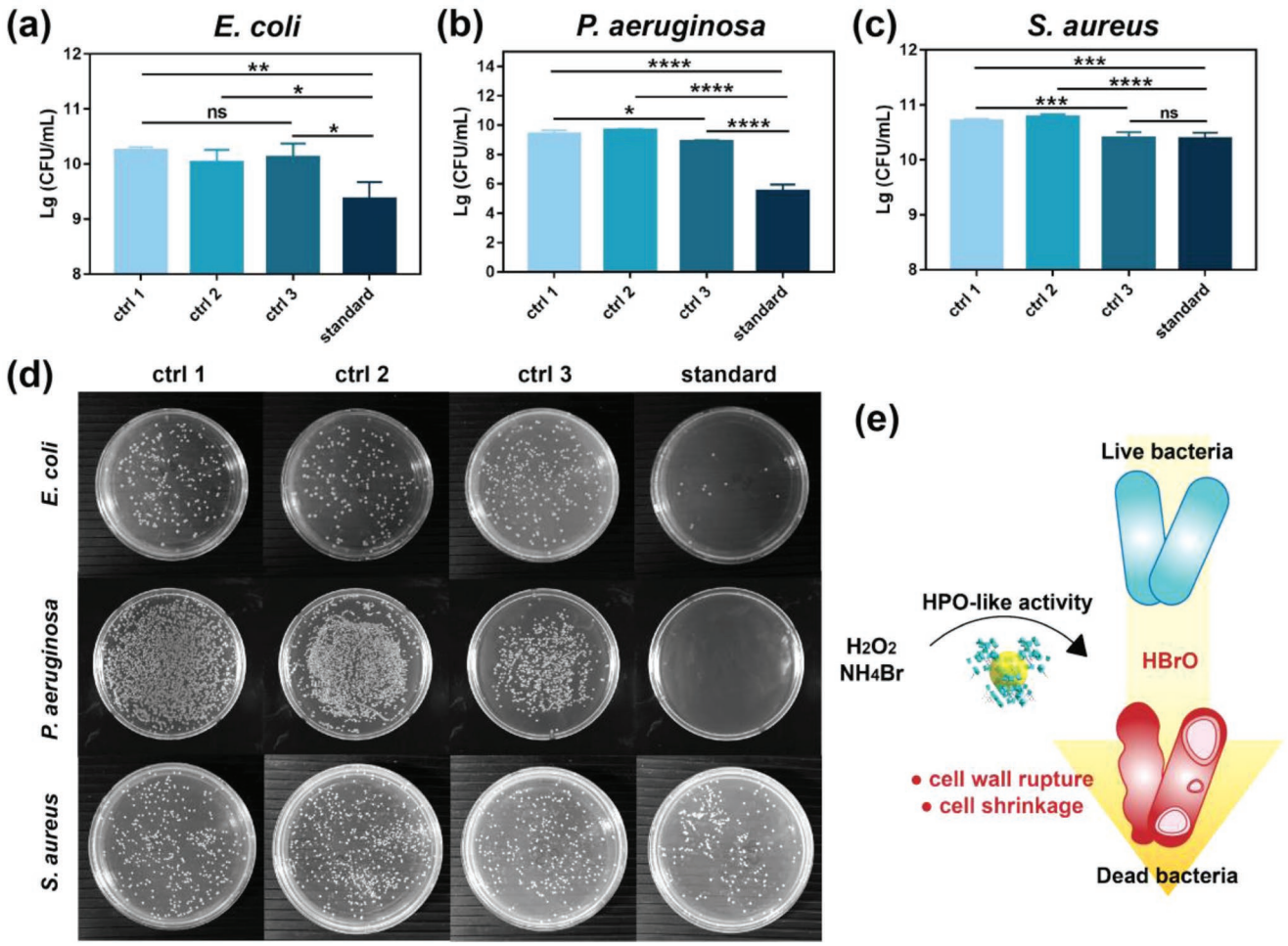

Figure 3. Antibacterial activity of Ce-MOF-808. Histograms of the colony forming units per milliliter (CFU/mL) of a) *E. coli*, b) *P. aeruginosa* and c) *S. aureus* after different treatments. d) Digital images of bacterial colonies of *E. coli*, *P. aeruginosa* and *S. aureus* after different treatments. ctrl 1: Bacteria in 0.9% NaCl; ctrl 2: Bacteria treated with 25×10^{-3} M NH_4Br and 1×10^{-3} M H_2O_2 in 0.9% NaCl; ctrl 3: Bacteria treated with 100 µg/mL Ce-MOF-808 in 0.9% NaCl; standard: Bacteria treated with 25×10^{-3} M NH_4Br, 1×10^{-3} M H_2O_2 and 100 µg/mL Ce-MOF-808 in 0.9% NaCl. (e) Schematic illustration of the possible antibacterial mechanism. Data are presented as mean ± SD (n = 4). Results were analyzed by student's *t*-test for two-group differences: *p < 0.05, **p < 0.01, ***p < 0.001, ****p < 0.0001 and ns (no significance).

the antibacterial effect of Ce-MOF-808 based on its HPO-like activity, which is illustrated in Figure 3e. It was obvious that *P. aeruginosa* in the standard group almost lost contact bacterial structure, exhibiting flat, distorted and irregular shapes (Figure S11, Supporting Information), which was consistent with the antibacterial results in Figure 3b.

Additionally, the antibacterial abilities of V_2O_5 NWs, CeO_2 NRs, and Ce-MOF-808 were compared under the same conditions (Figure S8, Supporting Information). CeO_2 NR is an admiring antifoulant[20] and indeed exhibited strong antibacterial ability toward *E. coli* and *S. aureus*. The ointment is that the antibacterial effect on *P. aeruginosa* based on the HPO-like activity of CeO_2 NRs was slightly weaker than those of Ce-MOF-808 and V_2O_5 NWs. There were few or no surviving bacteria in the ctrl 3 groups (bacteria + catalyst) treated with V_2O_5 NWs only, revealing that V_2O_5 NWs themselves exhibited a strong bactericidal ability. Similar results were observed in standard groups of V_2O_5 NWs, which was mainly due to its intrinsic antibacterial activity rather than its HPO-like activity. Additionally, it was reported that V_2O_5 NWs were too toxic to be further applied due to the leaching of metal ions.[21] Ce-MOF-808, by contrast, exhibited feeble intrinsic bactericidal effects on bacteria, but still inhibited bacterial growth effectively based on its HPO-like activity, making it another potential choice for antifouling in addition to CeO_2 NRs.

2.4. Oxidative Bromination of AHLs Catalyzed by Ce-MOF-808

Vanadium bromoperoxidase secreted by marine algae is capable of catalyzing the oxidative bromination process,[26] turning AHLs (Figure S10, Supporting Information), a kind of QS signaling molecule used by Gram-negative bacteria, into their brominated products, which further impedes bacterial intercellular communication.[27] Once the QS process is obstructed, individual microorganisms have trouble gathering and forming their aggregations, the biofilms. *P. aeruginosa* is one of the representative Gram-negative bacteria that utilize

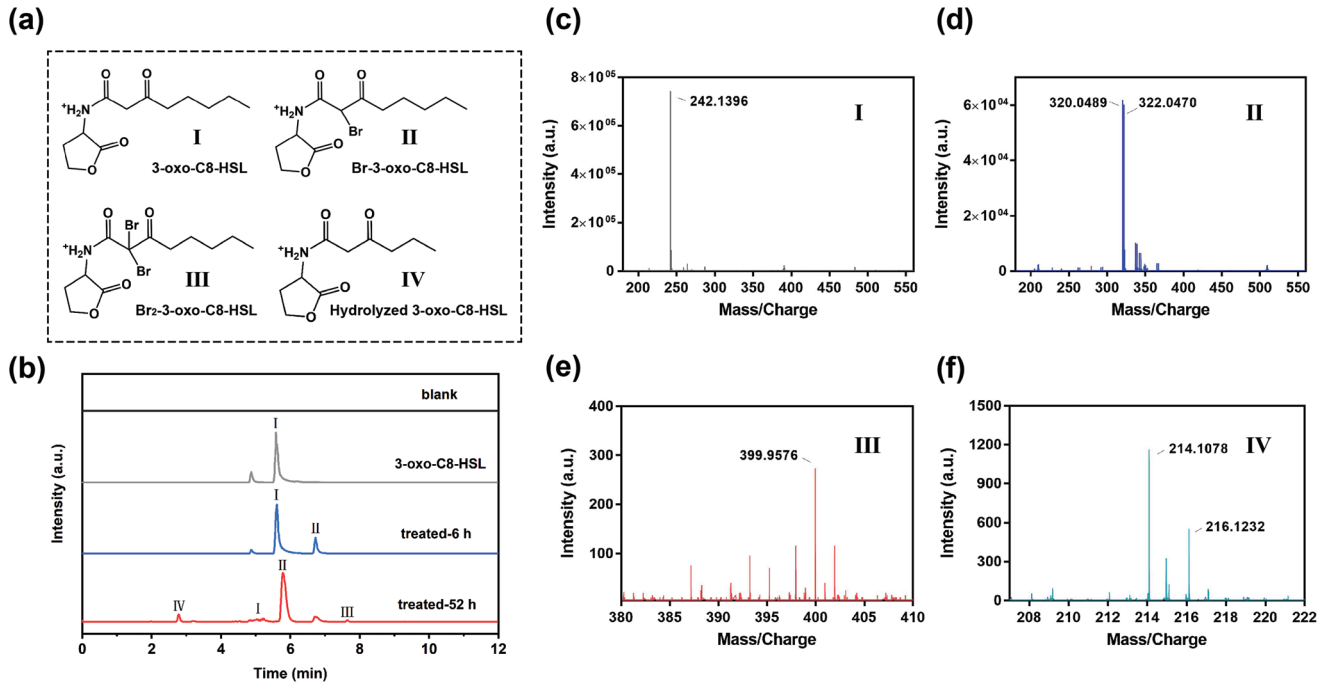

Figure 4. Products analysis of Ce-MOF-808 catalyzed the oxidative bromination process of *N*-(3-oxooctanoyl)-L-homoserine lactone (3-oxo-C8-HSL). a) Chemical structures of (I) 3-oxo-C8-HSL, (II) Br-3-oxo-C8-HSL, (III) Br_2-3-oxo-C8-HSL and (IV) hydrolyzed 3-oxo-C8-HSL. b) Total ion chromatogram (LC-MS) of the oxidative bromination reaction catalyzed by Ce-MOF-808 for 6 h or 52 h (1 mM 3-oxo-C8-HSL, 200 μg mL^{-1} Ce-MOF-808, 20×10^{-3} M NaBr and 20×10^{-3} M H_2O_2 for 6 h; 1×10^{-3} M 3-oxo-C8-HSL, 25 μg mL^{-1} Ce-MOF-808, 200×10^{-3} M NaBr and 500×10^{-3} M H_2O_2 for 52 h). Mass spectra of substrate c) and possible products d–e) corresponding to I-IV in a).

AHLs as QS signaling molecules,[15] while *E. coli* has two QS signaling molecule modulating systems, both AHLs and autoinducer-2.[28]

Since Ce-MOF-808 has been proven to possess HPO-like activity, we then verified whether Ce-MOF-808 could catalyze the oxidative bromination reaction of AHLs. In this study, we used one of the AHLs, *N*-(3-oxooctanoyl)-L-homoserine lactone (3-oxo-C8-HSL), as the model. Liquid chromatography–mass spectrometry (LC–MS) was utilized for analysis. **Figure 4**a illustrates the chemical structure of 3-oxo-C8-HSL and the possible chemical structures of the reaction products after catalysis. Mass spectrometer analysis is unable to provide exact information on molecular chemical structures, so the possible structures of brominated products were based on a previous report stating that HBrO is more likely to electrophilically halogenate at the carbon 2 of 3-oxo-C8-HSL (Figure S9, Supporting Information).[21] The total ion chromatogram in Figure 4b confirmed the formation of brominated products of 3-oxo-C8-HSL. The molecular weights of the reaction products analyzed by mass spectrometry were in accordance with their exact masses (Figure 4c–f), Table S2, Supporting Information). Additionally, a hydrolyzed fragment was also detected in the reaction mixture (Figure 4b,f). Whether the fragment was generated by the self-hydrolysis process of 3-oxo-C8-HSL or the hydrolysis process catalyzed by Ce-MOF-808 remains to be explored. In general, Ce-MOF-808 was verified to have a certain catalytic ability for the oxidative bromination of AHLs, providing new insight into the halogenation industry and pharmacy, not just surface-adhered biofilm treatment.

2.5. Ce-MOF-808 for Hindering Biofilm Formation

Biofilm formation is an indispensable link during surface biofouling in water; thus, its eradication is profoundly significant to fouling management.[6a,29] Based on the excellent broad-spectrum antibacterial property and AHL bromination effect of Ce-MOF-808, we continued to study its biofilm inhibition ability toward Gram-negative bacteria. During the formation of biofilms, Ce-MOF-808 and two substrates needed for the oxidative bromination reaction were incubated with bacterial suspensions under static conditions for 64 h (37 °C). Before the follow-up staining and observation, three washes were crucial for preventing the staining of planktonic cells. Confocal laser scanning microscopy (CLSM) and SEM were applied to observe biofilms. **Figure 5**a,b demonstrates that Ce-MOF-808 was a fierce threat to the biofilms formed by Gram-negative bacteria. Compared with the other 3 control groups, only one-fifth of biofilms formed successfully in the standard group of *E. coli*, and thinner biofilms formed in the standard groups of both *E. coli* and *P. aeruginosa*. The biomass of biofilms in the standard groups was also less than that in the control groups in crystal violet staining assays, as shown in Figure 5e,f. We ascribed these results to the synergistic effects of the antibacterial and QQ abilities of Ce-MOF-808 toward Gram-negative bacteria.

Furthermore, we also explored whether Ce-MOF-808 could inhibit the biofilm formation of *S. aureus*, a representative of Gram-positive bacteria. We observed that the biomass of biofilm formed in the standard group was much less than that in the other three control groups (Figure 5c), which was in line

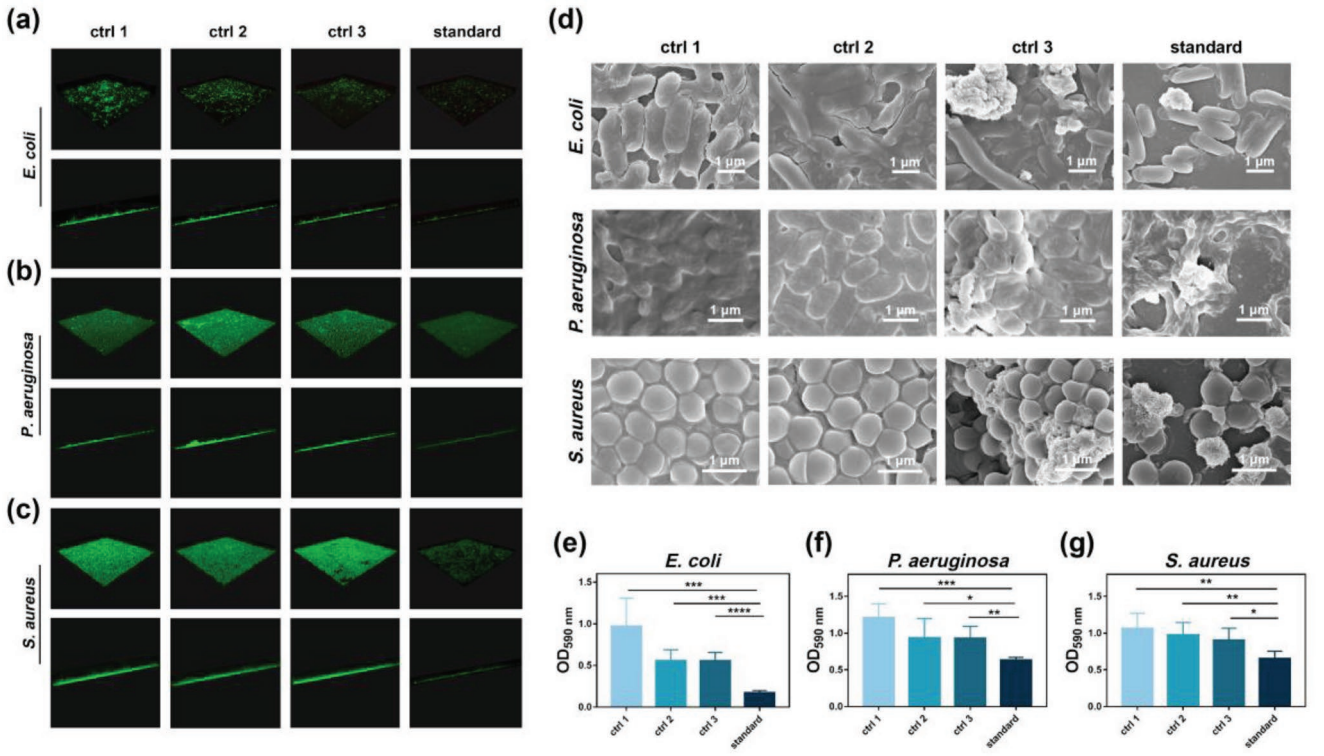

Figure 5. Anti-biofilm activity of Ce-MOF-808 based on its haloperoxidase-like activity. CLSM images of biofilms formed by (a) E. coli, (b) *P. aeruginosa* and (c) *S. aureus* after different treatments. (d) SEM images of biofilms formed by E. coli, *P. aeruginosa* and *S. aureus* after different treatments. Crystal violet staining of biofilms formed by (e) *E. coli*, (f) *P. aeruginosa* and (g) S. aureus after different treatments. ctrl 1: Bacteria in LB medium; ctrl 2: Bacteria treated with 25×10^{-3} M NH_4Br (5×10^{-3} M for CLSM experiments) and 1×10^{-3} M H_2O_2 (50×10^{-6} M for CLSM experiments) in LB medium; ctrl 3: Bacteria treated with 100 μg mL^{-1} Ce-MOF-808 in LB medium; standard: Bacteria treated with 25×10^{-3} M NH_4Br (5×10^{-3} M for CLSM experiments), 1×10^{-3} M H_2O_2 (50×10^{-6} M for CLSM experiments) and 100 μg mL^{-1} Ce-MOF-808 in LB medium. Data are presented as mean ± SD (n = 5). Results were analyzed by student's *t*-test for two-group differences: $^*p < 0.05$, $^{**}p < 0.01$, $^{***}p < 0.001$.

with the semiquantitative result in Figure 5g. This inspiring result signified that Ce-MOF-808 could also inhibit the formation of Gram-positive bacterial biofilms. Combining slightly weaker antibacterial effects on Gram-positive bacteria than Gram-negative bacteria, we inferred that Ce-MOF-808 might also deactivate the QS signaling molecule of Gram-positive bacteria, which needs to be further confirmed.

The biomasses of biofilms in the ctrl 3 groups (bacteria + Ce-MOF-808) of these three kinds of bacteria were less than those of the ctrl 1 groups (bacteria), which was due to the intrinsic hydrolytic activity of MOF-808.[30] The SEM images in Figure 5d further confirmed that the HPO-like activity and hydrolytic activity of Ce-MOF-808 synergistically hindered biofilm formation. The SEM images in Figure S12 (Supporting Information) show the conspicuous surface-adhered biofilm combatting performance and bactericidal effect of Ce-MOF-808 again. Taken together, Ce-MOF-808 with HPO-like activity had a certain effect on inhibiting surface-adhered biofilm formation, shedding new light on surface biofouling management.

2.6. Ce-MOF-808 Inhibits the Formation of Pipes-Adhered Biofilm

To investigate the antibiofilm effect of Ce-MOF-808 on biofilms adhering to water pipes, we further built a pipe-adhered biofilm model. Bacteria were seeded in polyvinyl chloride pipe elbows and grown for 64 h under dark, static conditions to form biofilms. To quantitatively analyze the antibiofilm effects based on the HPO-like activity of Ce-MOF-808, bacterial cells adhered to the pipe surfaces were removed by sterile cotton swabs after discarding bacterial suspensions. The cotton swabs were then transferred to 2 mL of sterile 0.9% NaCl solution, followed by vortexing and dilution for agar plate spreading (**Figure 6**a). The plate counting results are shown in Figure 6b. The numbers of bacterial colonies in the standard groups were much lower than those in the other three control groups. Histograms of CFU/mL in Figure 6c–e also demonstrated that Ce-MOF-808 was able to inhibit the formation of biofilms in water pipes in the presence of Br^- and H_2O_2, making it possible to be applied for water pipe cleaning.

3. Conclusions

In summary, as a new HPO-like enzyme mimic, easily fabricated Ce-MOF-808 has the ability to catalyze the oxidative bromination of the Gram-negative bacterial QS signaling molecule AHL to form its brominated product, hampering the QS mechanism and hence suffocating the formation of biofilms. Given this high HPO-like activity, Ce-MOF-808 was developed to kill

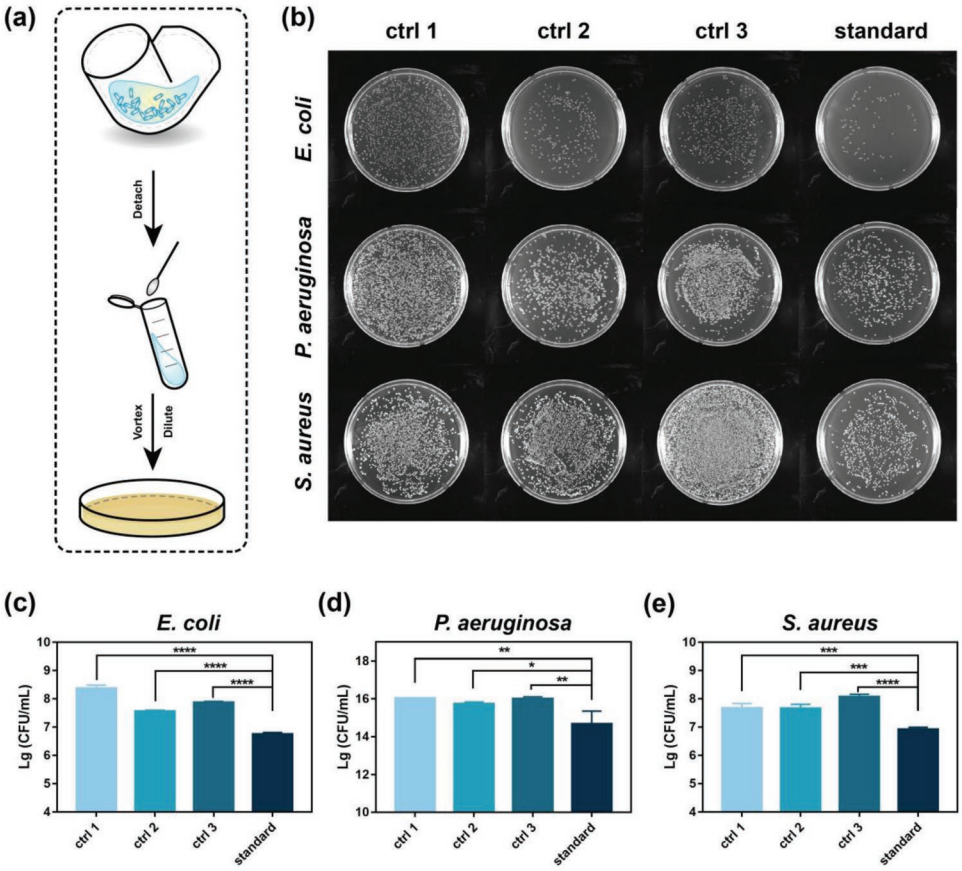

Figure 6. The inhibition effects of Ce-MOF-808 on the biofilm adhered to the inner surface of the water pipe. (a) Scheme of the experimental steps for quantitative analysis of the residual bacterial cells adhered to the inner wall of the water pipe. (b) Digital images of bacterial colonies of *E. coli*, *P. aeruginosa* and *S. aureus* after different treatments. Histograms of CFU/mL of (c) *E. coli*, (d) *P. aeruginosa* and (e) *S. aureus* after different treatments. The culture medium was diluted in a ratio of 1:3 (LB:water). ctrl 1: Bacteria; ctrl 2: Bacteria treated with 25×10^{-3} M NH_4Br and 1×10^{-3} M H_2O_2; ctrl 3: Bacteria treated with 100 μg mL^{-1} Ce-MOF-808; standard: Bacteria treated with 25×10^{-3} M NH_4Br, 1×10^{-3} M H_2O_2 and 100 μg mL^{-1} Ce-MOF-808. Data are presented as mean ± SD (n = 4). Results were analyzed by student's *t*-test for two-group differences: $*p < 0.05$, $**p < 0.01$, $***p < 0.001$, $****p < 0.0001$.

both Gram-negative and Gram-positive bacteria. In addition, an antibiofilm study proved that Ce-MOF-808 was an extraordinary inhibitor of biofilm formation by virtue of its antibacterial activity and QS disruption ability. Along with its outstanding enzyme-like activity, Ce-MOF-808 also had favorable performance in long-term stability, recyclability, and biosafety. The finding of the HPO-like activity of Ce-MOF-808 expanded the initially limited range of HPO-like mimics, facilitating substitution with natural HPO to hinder pipe-adhered biofilm formation. Furthermore, it provided wide applicable possibilities of Ce-MOF-808 in infectious diseases, food contamination, and biofouling treatments.

Supporting Information

Supporting Information is available from the Wiley Online Library or from the author.

Acknowledgements

Z.Z. and S.L. contributed equally to this work. This work was supported by the National Key R&D Program of China (2019YFA0709200 and 2021YFF1200700), the National Natural Science Foundation of China (21874067 and 21722503), Jiangsu Provincial Key R&D Program-Social Development, the CAS Interdisciplinary Innovation Team (JCTD-2020-08), the PAPD Program, and Fundamental Research Funds for the Central Universities (021314380195).

Conflict of Interest

The authors declare no conflict of interest.

Data Availability Statement

The data that support the findings of this study are available from the corresponding author upon reasonable request.

Keywords

biofilms, haloperoxidase mimics, metal–organic frameworks, oxidative bromination, quorum sensing

Received: June 2, 2022
Revised: June 29, 2022
Published online:

[1] a) J. W. Costerton, P. S. Stewart, E. P. Greenberg, *Science* **1999**, *284*, 1318; b) K. P. Rumbaugh, K. Sauer, *Nat. Rev. Microbiol.* **2020**, *18*, 571; c) H. C. Flemming, J. Wingender, U. Szewzyk, P. Steinberg, S. A. Rice, S. Kjelleberg, *Nat. Rev. Microbiol.* **2016**, *14*, 563; d) D. Davies, *Nat Rev Drug Discov* **2003**, *2*, 114.
[2] A. Syafiuddin, R. Boopathy, M. A. Mehmood, *Bioresource Technol Rep* **2021**, *15*, 100745.
[3] A. Bridier, P. Sanchez-Vizuete, M. Guilbaud, J. C. Piard, M. Naitali, R. Briandet, *Food Microbiol.* **2015**, *45*, 167.
[4] J. Antunes, P. Leao, V. Vasconcelos, *Environ Microbiol Rep* **2019**, *11*, 287.
[5] X. Xiong, Y. Huang, C. Lin, X. Y. Liu, Y. Lin, *Nanoscale* **2019**, *11*, 22206.
[6] a) M. Lejars, A. Margaillan, C. Bressy, *Chem. Rev.* **2012**, *112*, 4347; b) H. Yan, Q. Wu, C. Yu, T. Zhao, M. Liu, *Adv. Mater. Interfaces* **2020**, *7*, 2000966.
[7] a) T. Yimyai, R. Thiramanas, T. Phakkeeree, S. Iamsaard, D. Crespy, *Adv. Funct. Mater.* **2021**, *31*, 2102568; b) W. Wang, Y. Lu, H. Zhu, Z. Cao, *Adv. Mater.* **2017**, *29*, 1606506.
[8] a) D. P. Linklater, V. A. Baulin, S. Juodkazis, R. J. Crawford, P. Stoodley, E. P. Ivanova, *Nat. Rev. Microbiol.* **2021**, *19*, 8; b) S. Rigo, C. Cai, G. Gunkel-Grabole, L. Maurizi, X. Zhang, J. Xu, C. G. Palivan, *Adv. Sci.* **2018**, *5*, 1700892.
[9] a) Y. Yang, X. Wu, C. He, J. Huang, S. Yin, M. Zhou, L. Ma, W. Zhao, L. Qiu, C. Cheng, C. Zhao, *ACS App Mater Inter* **2020**, *12*, 13698; b) J. M. V. Makabenta, A. Nabawy, S. S. Malan, R. Patel, V. M. Rotello, C.-H. Li, *Nat. Rev. Microbiol.* **2021**, *19*, 23.
[10] J. B. Kristensen, R. L. Meyer, B. S. Laursen, S. Shipovskov, F. Besenbacher, C. H. Poulsen, *Biotechnol. Adv.* **2008**, *26*, 471.
[11] a) H. Wei, E. Wang, *Chem. Soc. Rev.* **2013**, *42*, 6060; b) J. Wu, X. Wang, Q. Wang, Z. Lou, S. Li, Y. Zhu, L. Qin, H. Wei, *Chem. Soc. Rev.* **2019**, *48*, 1004; c) Y. Huang, J. Ren, X. Qu, *Chem. Rev.* **2019**, *119*, 4357; d) M. Liang, X. Yan, *Acc. Chem. Res.* **2019**, *52*, 2190; e) G. Tang, J. He, J. Liu, X. Yan, K. Fan, *Exploration* **2021**, *1*, 75.
[12] a) Z. Chen, Z. Wang, J. Ren, X. Qu, *Acc. Chem. Res.* **2018**, *51*, 789; b) L. Mei, S. Zhu, Y. Liu, W. Yin, Z. Gu, Y. Zhao, *Chem. Eng. J.* **2021**, *418*, 129431; c) X. Xiong, Y. Huang, C. Lin, X. Y. Liu, Y. Lin, *Chem. Commun.* **2019**, *11*, 22206.
[13] a) Y. Huang, Y. Liu, S. Shah, D. Kim, A. Simon-Soro, T. Ito, M. Hajfathalian, Y. Li, J. C. Hsu, L. M. Nieves, F. Alawi, P. C. Naha, D. P. Cormode, H. Koo, *Biomaterials* **2021**, *268*, 120581; b) Z. Liu, F. Wang, J. Ren, X. Qu, *Biomaterials* **2019**, *208*, 21.
[14] Z. Chen, H. Ji, C. Liu, W. Bing, Z. Wang, X. Qu, *Angew Chem Int Edit* **2016**, *55*, 10732.
[15] K. Lee, H. Yu, X. Zhang, K. H. Choo, *Bioresource Technol* **2018**, *270*, 656.
[16] C. Leblanc, et al., *Coordin Chem Rev* **2015**,*134*, 301.
[17] A. Butler, M. Sandy, *Nature* **2009**, *460*, 848.
[18] H.-S. Oh, C.-H. Lee, *J Membrane Sci* **2018**, *554*, 331.
[19] a) P. Adak, B. Ghosh, B. Pakhira, R. Sekiya, R. Kuroda, S. K. Chattopadhyay, *Polyhedron* **2017**, *127*, 135; b) T. L. Fernández, E. T. Souza, L. C. Visentin, J. V. Santos, A. S. Mangrich, R. B. Faria, O. A. C. Antunes, M. Scarpellini, *J. Inorg. Biochem.* **2009**, *103*, 474; c) F. Natalio, R. André, A. F. Hartog, B. Stoll, K. P. Jochum, R. Wever, W. Tremel, *Nat. Nanotechnol.* **2012**, *7*, 530.
[20] K. Herget, P. Hubach, S. Pusch, P. Deglmann, H. Götz, T. E. Gorelik, I. A. Gural'skiy, F. Pfitzner, T. Link, S. Schenk, M. Panthöfer, V. Ksenofontov, U. Kolb, T. Opatz, R. André, W. Tremel, *Adv. Mater.* **2017**, *29*, 1603823.
[21] K. Herget, H. Frerichs, F. Pfitzner, M. N. Tahir, W. Tremel, *Adv. Mater.* **2018**, *30*, 1707073.
[22] a) M. Li, J. Chen, W. Wu, Y. Fang, S. Dong, *J. Am. Chem. Soc.* **2020**, *142*, 15569; b) J. Wu, Z. Wang, X. Jin, S. Zhang, T. Li, Y. Zhang, H. Xing, Y. Yu, H. Zhang, X. Gao, H. Wei, *Adv. Mater.* **2021**, *33*, 2005024.
[23] H.-Y. Wang, X.-W. Hua, H.-R. Jia, C. Li, F. Lin, Z. Chen, F.-G. Wu, *ACS Biomater. Sci. Eng.* **2016**, *2*, 987.
[24] G. J. Colpas, B. J. Hamstra, J. W. Kampf, V. L. Pecoraro, *J. Am. Chem. Soc.* **1996**, *118*, 3469.
[25] J. Huang, J. Zhou, J. Zhuang, H. Gao, D. Huang, L. Wang, W. Wu, Q. Li, D.-P. Yang, M.-Y. Han, *ACS Appl Mater Inter* **2017**, *9*, 36606.
[26] R. Wever, M. A. van der Horst, *Dalton Trans* **2013**, *42*, 11778.
[27] C. M. Waters, B. L. Bassler, *Annu. Rev. Cell Dev. Biol.* **2005**, *21*, 319.
[28] M. M. Kendall, V. Sperandio, *EcoSal Plus* **2014**, *6*, 2013.
[29] M. S. Selim, M. A. Shenashen, S. A. El-Safty, S. A. Higazy, M. M. Selim, H. Isago, A. Elmarakbi, *Prog. Mater. Sci.* **2017**, *87*, 1.
[30] a) S. Dai, C. Simms, I. Dovgaliuk, G. Patriarche, A. Tissot, T. N. Parac-Vogt, C. Serre, *Chem. Mater.* **2021**, *33*, 7057; b) E. Palmajumder, S. R. Dash, J. Mitra, K. K. Mukherjea, *ChemistrySelect* **2018**, *3*, 7429.